

## PROGRESS IN MAGNET SYSTEM FOR THE SPRING-8 STORAGE RING

J. Ohnishi, Y. Oikawa, and S. Motonaga  
RIKEN-JAERI Synchrotron Radiation Facility Design Team  
2-28-8 Honkomagome, Bunkyo-ku, Tokyo 113 Japan

### Abstract

The first-step design of a dipole, quadrupole, and sextupole magnet for the Spring-8 storage ring has been finished, and the more detailed design is in progress. At the same time, the prototypes of these magnets are under construction. This paper describes the mechanical design, and field quality calculated by means of 2-dimensional numerical program.

### Introduction

The storage ring of Spring-8 is being designed by RIKEN to be a highly-brilliant synchrotron-radiation source.<sup>1</sup> It was designed in Chasman-Green lattice to get an emittance lower than  $10^{-8}$  mrad. The ring is 1437 m around, containing 48 unit cells. The layout of a cell is shown in Fig.1. Four cells located symmetrically have no bending magnet, because long straight sections are considered for special insertion devices. Those sections can be made by a rearrangement of the magnets in future.

Magnet system contains 88 dipole, 480 quadrupoles, and 336 sextupoles. There are also 576 dipole correctors; 364 of them are incorporated with the dipoles or sextupoles by the addition of extra windings, 96 of them individual horizontal correctors,

and 96 of them for both vertical and horizontal corrections. Furthermore, three septum magnets and four kickers are accommodated for beam injection.<sup>2</sup> All the magnets except for several pulse magnets are operated statically (dc operation), because the beam is injected after accelerated up to the nominal energy (8 GeV) in the booster synchrotron.<sup>3</sup>

The required field qualities for the dipole, quadrupole, and sextupole magnets are very stringent as shown in Table 1 since this storage ring is supposed to have extremely low emittance beam. Therefore, we have designed the pole geometry of magnet carefully by carrying out numerical calculations of magnetic fields with two-dimensional programs, LINDA<sup>4</sup> and TRIM<sup>5</sup>.

Each magnet itself is assembled from a stacked core which is a 0.5 mm thick silicon-steel plate and stainless steel end plates of 25 mm (20 mm) thick. The choice of laminated structure was made in the aspects of the identity in magnetic field quality, and construction cost.

At present, full-scale prototypes of dipoles, quadrupoles, and sextupoles are being built in order to verify the designs by measuring the magnetic fields. They will be also used to improve the construction techniques. Moreover, a design of power supply system<sup>6</sup> for the magnets is under way, together with the development of high accuracy field-measurement systems.

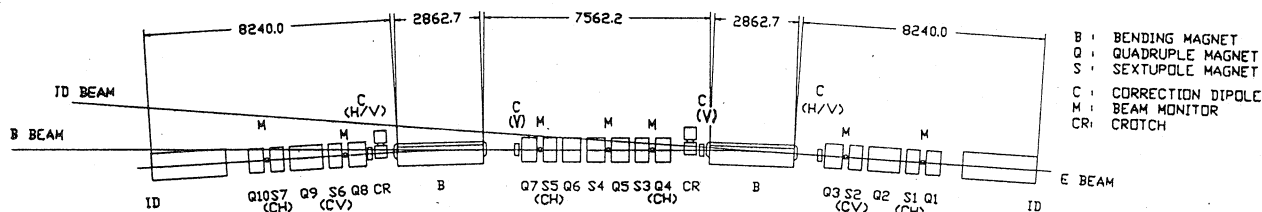


Fig.1 An arrangement of dipole, quadrupole, sextupole, and correction magnets in a cell of the storage ring

**Table 1.**  
Required field quality of dipole, quadrupole, and sextupole magnets

Magnet	Dipole	Quadrupole	Sextupole
Maximum field strength	0.655 T	18 T/m	360 T/m <sup>2</sup>
Gap distance or bore radius	65 mm	45 mm	55 mm
Effective field length	2.863 m	0.5, 0.6, 1.1 m	0.6, 0.45 m
Field uniformity	$\Delta B1/B1$	$\Delta G1/G1$	$\Delta G1/G1$
	$<5 \times 10^{-4}$	$<5 \times 10^{-4}$	$<1 \times 10^{-3}$
Region size	$x=\pm 140$ mm $y=\pm 17$ mm	$x=\pm 135$ mm $y=\pm 15$ mm	$x=\pm 135$ mm $y=\pm 15$ mm

### Dipole magnet

The cross-sectional view of a dipole magnet are shown in Fig.2. A C-shaped rectangular configuration has been chosen because of the following reasons; it is easy and economic to construct and also easy to accommodate beam chambers and to measure the field.

The height of gap was determined as 65 mm, which provides 40 mm for beam clear space in a vacuum chamber, and 7 mm x 2 for the chamber wall thickness, 2 mm x 2 for the thermal insulation, and finally 3 mm for a clearance at radial shims (2 mm x 2). The pole width was 240 mm to insure the high-quality horizontal field region of 106 mm including a sagitta of 26 mm.

The geometrical accuracy of the finished core is deduced to be within  $\pm 0.02$  mm for the gap height, and  $\pm 1$  mm for the magnet length from the measurement on the prototype.

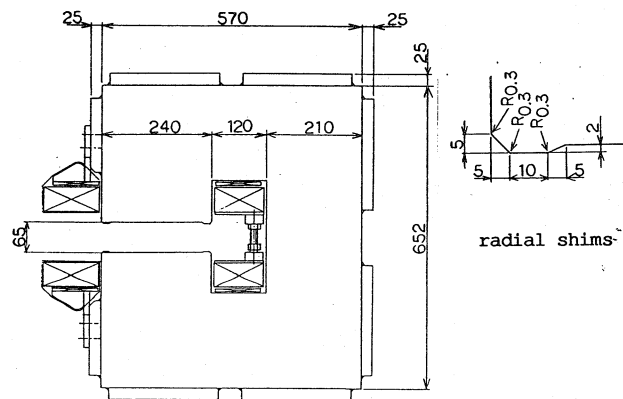


Fig.2 The cross-sectional view of a dipole magnet

The calculated field distribution of a dipole magnet is shown in Fig.3. The maximum deformation of the poles due to the magnetic force, which appears as a reduction of the gap, was estimated to be about 10  $\mu$ m by a simple FEM. This value is as small as the geometrical core accuracy, and the corresponding change in the field distribution is also small enough as shown in Fig.3.

The coils of dipole are composed of main and auxiliary ones. The main coils are constructed to be two pancakes of 14 mm x 23 mm copper conductor with a cooling channel of 10 mm diameter. On the other hand, the auxiliary coils are capable of providing a

Table 2  
Main magnets parameters

	Dipole	Quadrupole			Sextupole	
Number of magnets	88	192	192	96	288	48
Maximum strength	0.655 T		18 T/m		300 T/m <sup>2</sup>	360 T/m <sup>2</sup>
Effective length (m)	2.86	0.5	0.6	1.1	0.45	0.6
Gap or Bore radius (mm)	65		45		55	
Magnetomotive force (AT)	$3.5 \times 10^4$		$1.5 \times 10^4$		$7.0 \times 10^3$	$8.3 \times 10^3$
Turns per pole	14		16		22	
Conductor size (mm)	$14 \times 23 - \phi 10$		$11.5 \times 16 - \phi 5$		$8 \times 8 - \phi 3.5$	$\phi 4.0$
Current (A)	1250		940		320	380
Current density (A/mm <sup>2</sup> )	5.1		5.8		5.9	7.0
Voltage (V)	20.3	10.8	13.0	23.8	18.3	27.2
Power (KW)	25.3	10.2	12.2	22.4	5.9	10.3
Cooling water circuits	2	4	4	8	6	6
Water flow (l/min)	18.1	7.3	8.7	16.0	4.2	7.4
Pressure drop (bar)	5.0	2.0	3.2	2.6	2.3	4.1
Temperature rise (°C)	20		20			20

magnetomotive force of 600 [AT] at air cooling. They will be employed to compensate for a random error in magnetic strength ( $B \times l$ ) from one magnet to another, and also for COD correction.

The major parameters of dipole magnets are given in Table 2.

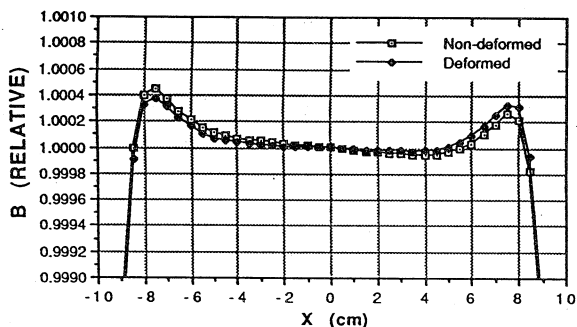


Fig.3 Calculated transversal field distributions of a dipole magnet normalized at  $x=0$  ( $B=0.655$  T). Deformation due to the magnetic force is considered for one case.

#### Quadrupole magnet

The cross-sectional view and pole profile of a quadrupole magnet are shown in Fig.4. All the quadrupole magnets in the storage ring are same in their cores except the lengths. There exist three different lengths; 0.5 m, 0.6 m, 1.1 m. The bore diameter (90 mm) was decided based on the size of beam chamber, and the uniform field region. The upper and lower halves of the magnet are separated magnetically. They are joined through stainless steel parts, because the structure of joint parts is supposed to be different depending on the location to provide space

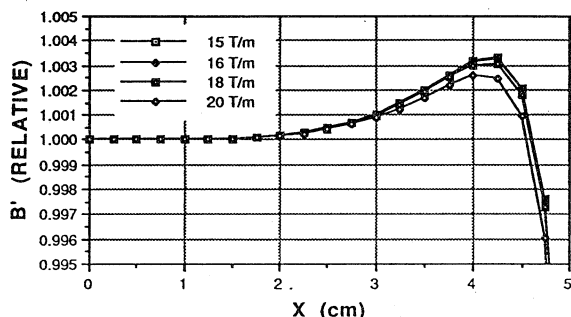


Fig.5 Calculated distributions of the field gradient ( $B'$ ) of a quadrupole magnet for the several strengths

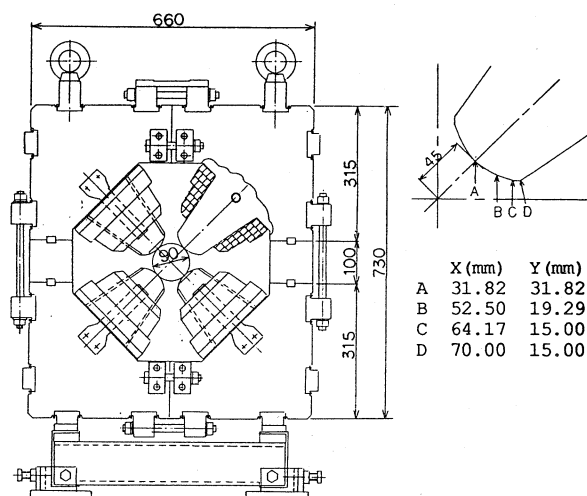


Fig.4 The cross section and pole profile of a quadrupole magnet

for a photon beam line. The magnetic core geometry of all the quadrupoles can be, thus, kept identical. On the other hand, the mechanical design of joints has not been completed yet.

The calculated distributions of field gradient ( $B'$ ) are shown in Fig.5 along a radial direction. An adjustment by a shape of radial shims was also included so that the  $B'$  strengths are intensified along the radial direction as indicated in Fig.5. The reason is that an integrated gradient over the magnet is presumed to be decreased along the direction. The integrated gradient distribution can be corrected simply by adding end shims if necessary.

It is desirable that all the quadrupoles are operated within gradient strengths of 16 and 18 T/m for the normal operation and the maximum, respectively, because they are satisfied with the severe required field quality (see Table 1). But we believe that a possibility of the maximum strength should be verified by measuring the real field of the prototype for the sake of shorter magnet length.

The major parameters are listed in Table 2.

#### Sextupole magnet

Seven sextupole magnets are placed in a unit cell; three of them correct chromaticities and the remaining four extend the beam dynamic aperture. Furthermore, it is planned that most of sextupoles in the ring provide even a horizontal or vertical dipole field to steer the beam by adding special coils to them. An arrangement of the sextupoles in a cell and their field strength in a nominal mode are shown in Table 4.

**TABLE 3.**  
Family of sextupole magnets

	S1 (S1)	S2 (S2)	SD (S3)	SF (S4)	SD (S5)	S3 (S6)	S4 (S7)
B* (T/m <sup>2</sup> )	210	-239	-259	347	-259	-178	286
L <sub>eff</sub> (m)	0.45	0.45	0.45	0.60	0.45	0.45	0.45
Steering	H	V	H	None	H	V	H

H: Horizontal steering coils are incorporated  
V: Vertical steering coils are incorporated

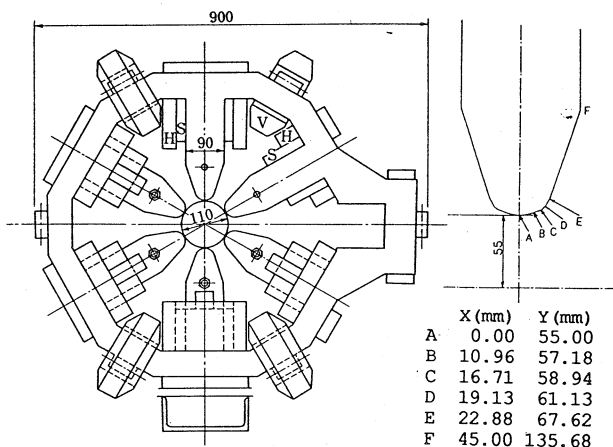


Fig. 6 The cross section and pole profile of a sextupole magnet

Two different types have been designed in yoke structure: One is completely symmetric and the other asymmetric. Fig. 6 shows a cross-sectional view of the sextupole magnet, which has the asymmetrical yoke structure. This is due to an extra room for the extraction of a photon beam. The bore diameter is 110 mm. The contour for all the pole tips is the same,  $r_0^3 = r^3 \cos 3\theta$  with radial shims, as shown in Fig. 6. The widths of a pole and a yoke are designed to be thick enough so that the maximum strength of sextupole field can be excited up to 360 T/m<sup>2</sup> without any correction field, or 300 T/m<sup>2</sup> with a correction dipole field of 0.06 T. The major parameters of sextupole magnet are also listed in Table 2.

Fig. 7 shows the calculated field distributions of a sextupole magnet with asymmetrical yokes. The Y-axis indicates  $dBy/dx/x$  on a medium plane. Asymmetrical field distributions are caused by the core geometry, and originated from a quadrupole component. Its value was, however, estimated to be only  $1.3 \times 10^{-3}$  T/m, which is smaller than the gradient errors of a quadrupole magnet, suggesting no serious influence to a beam.

All the sextupole magnets except for 'SF' family have auxiliary coils for providing steering dipole fields. The coils are indicated by 'H' for horizontal

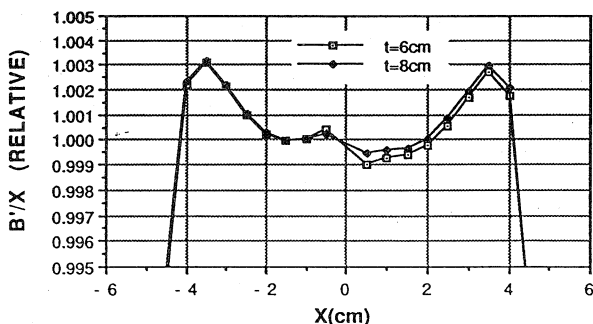


Fig. 7 Calculated distributions of the field gradient (B'/X) of a sextupole magnet with asymmetrical yokes. 't' indicates the thickness of an extended yoke.

**Table 4**  
Parameters of Steering Windings

	horiz.		vert.
	Coil A	Coil B	Coil C
Family	S1, S3, S5, S7		S2, S6
Number of magnets	192		96
Physical length (m)	0.45		0.45
Kick angle (mrad)	1.0		1.0
Peak field (T)	0.059		0.059
Number of coils	2	4	4
Turns per pole	340	136	275
Conductor size (mm <sup>2</sup> )	2.4 x 4		2.4 x 4
Current, max. (A)	12.4	12.4	9.5
Current density (A/mm <sup>2</sup> )	1.3	1.3	1.0
Voltage per coil (V)	12.6	5.1	7.3
Power per coil (W)	105	63	70

steering and 'V' for vertical in Fig. 6. In the actual magnets, either 'H' coils or 'V' coils are installed as in Table 3. Table 4 shows the parameters of steering windings. The maximum field strength is 0.06 T, which gives an 1 mrad kick to the beam, and is confirmed to be sufficient through a simulation of the COD correction.

Fig. 8 shows the calculated distributions of a horizontal and a vertical dipole field induced by the steering elements in a sextupole magnet. B<sub>x</sub>(y) on a x=0 plane is plotted for the horizontal fields, and B<sub>y</sub>(x) on a y=0 plane for the vertical. Though the dipole field is superimposed on the sextupole field in a actual magnet, the change in field distributions was hardly seen according to the 2-dimensional calculation.<sup>7</sup>

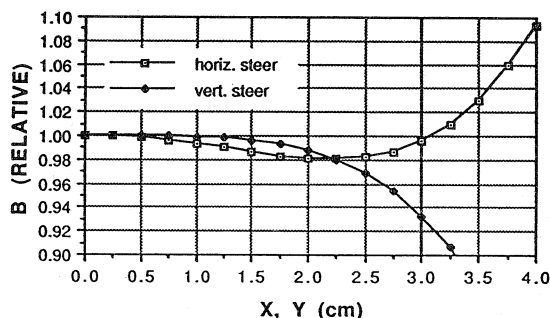


Fig. 8 Calculated distributions of steering dipole fields provided by correction elements incorporated with a sextupole magnet. Normalized at x=0 (0.06 T).

#### Conclusion

We have completed the preliminary design of a dipole, quadrupole, and sextupole magnet. At present, prototypes of these magnets are being built. We are planned to measure the characteristics of the prototypes and improve the design.

#### References

1. M.Hara, et al., Proc. of Particle Accelerator Conf., Chicago, U.S.A., 1989.
2. H.Miyade, et al., presented at this symposium
3. H.Yokomizo, et al., Proc. of Particle Accelerator Conf., Chicago, U.S.A., 1989.
4. K.Endo, et al., KEK Accelerator-1, 1972.
5. K.Endo, et al., KEK Accelerator-2, 1974.
6. H.Takebe, presented at this symposium
7. J.Ohnishi, Proc. of 11th Int. Conf. on Magnet Technology, Tsukuba, Japan, August, 1989.